

The stability of conical end caps with spherical tips as end closures for pressure vessels

Md. Raisuddin Khan & Md. Wahhaj Uddin

Mechanical Engineering Department, Bangladesh University of Engineering and Technology, Dhaka-1000, Bangladesh

(Received 19 April 1994; accepted 6 May 1994)

The instability under pressure of conical end caps with spherical tips when used as end closures to pressure vessels is studied in this paper. The spherical tip of the conical end cap was assumed to be attached in such a way that continuity of the slope at the cone/sphere junction was maintained. The geometrical parameters of the spherical-tip conical end closure are the ratio r/R ; the apex angle Ψ of the conical frustum; and the thickness ratio R/h , where r and R are respectively the radius of the cone at the sphere/cone and vessel/cone junctions and h is the thickness of the shell. Governing nonlinear differential equations of axisymmetric deformation which ensure the unique states of lowest potential energy under given pressure have been solved by using the method of multisegment integration, developed by Kalnins and Lestingi.¹ The results show that the critical pressure for the end closure decreases with increasing apex angle at constant values of R/h and r/R . At constant values of Ψ and R/h , the critical pressure remains constant over a considerable range of r/R and then decreases to a minimum value at $r/R = 1.0$ which corresponds to a purely spherical end cap without the conical extension.

NOTATION

C, D	Extensional rigidity Eh , bending rigidity $Eh^3/[12(1 - \nu^2)]$	P, \bar{P}, \bar{R}	External pressure, P/E , ξ_e/R
\bar{C}, \bar{D}	$(1 - \nu^2)\xi_e/R$, $1/\{12\bar{P}\bar{T}^2\bar{R}(1 - \nu^2)\}$	r_o, \bar{r}_o	Radial distance of points on undeformed middle surface from axis of symmetry, r_o/ξ_e
E, ν	Young's modulus, Poisson's ratio	r	$r_o + u$, also radius of the end closure at the cone/sphere junction
h, R	Shell thickness, radius at cone-vessel junction	u, w	Radial and axial displacements
H, V	Radial and axial stress resultants	\bar{u}, \bar{w}	uEh/PR^2 , wEh/PR^2
\bar{H}, \bar{V}	H/PR , V/PR	α, β	Shell parameter, $\phi_o - \phi$
k_θ, k_ξ	Circumferential and meridional curvature changes	$\epsilon_\xi, \epsilon_\theta$	Meridional and circumferential strains
$\bar{k}_\theta, \bar{k}_\xi$	$k_\theta\xi_e$, $k_\xi\xi_e$	$\bar{\epsilon}_\xi, \bar{\epsilon}_\theta$	$\epsilon_\xi Eh\xi_e/PR^2$, $\epsilon_\theta Eh\xi_e/PR^2$
\bar{L}, \bar{T}	$\xi_e Eh/PR^2$, R/h	ξ_e	Meridional length from the apex of the end closure to the cone/vessel junction
M_θ, M_ξ	Circumferential and meridional couple resultants	$\xi, \bar{\xi}$	Distance measured from apex along the meridian, ξ/ξ_e
$\bar{M}_\theta, \bar{M}_\xi$	M_θ/PRh , M_ξ/PRh	σ_{ci}, σ_{co}	Circumferential stress index at inner and outer surfaces
N_ξ, N_θ	Meridional and circumferential stress resultants	ϕ_o, ϕ	Angle between axis of symmetry and normal to undeformed and deformed middle surface
$\bar{N}_\xi, \bar{N}_\theta$	N_ξ/PR , N_θ/PR		

1 INTRODUCTION

Pressure vessels are usually made of segments of shells of different geometries such as cylinders, cones, spheres, ellipsoids, or some other exotic geometry. The end closures of these vessels are in most cases spherical, ellipsoidal, plate or conical in shapes. The end closures are usually the most vulnerable section of vessels both in terms of stresses and instability. Instability is becoming the overriding criterion in designing externally pressurised vessels with improving material and fabrication technology available today.

Until now very few works have been done on the stability of combinations of shells.²⁻⁵ In particular spherical cap top conical shells have not been investigated. Submarine and many other pressure-sustaining systems often use a hemispherical or a spherical cap as the end closure of cylindrical shells. In particular, spherical caps when combined with cylindrical shells develop sharp geometric discontinuity. This geometric discontinuity in turn develops high discontinuity stress, and makes the junction vulnerable. Moreover spherical caps are generally very weak in stability in comparison to conical caps. Considering these facts, it is expected that a conical frustum with a spherical tip would prove to be a superior end closure for pressure vessels. The present paper is thus devoted to the study of instability of spherical-tip conical end closures of pressure vessels. This is shown schematically in Fig. 1 which shows a spherical cap attached at the narrow end of a truncated conical shell without any discontinuity in slope at the junction.

2 ANALYSIS

Nonlinear governing equations for axisymmetric deformations of shells as developed by Reissner⁸

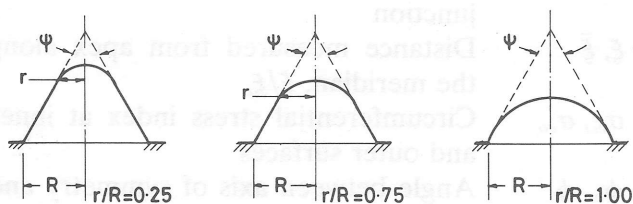


Fig. 1. Section through spherical cap-cone combination with different r/R ratio.

and modified by Uddin⁶ are solved by using the method of multisegment integration developed by Kalnins and Lestingi¹ with the help of the computer code developed by Uddin.⁷ The critical pressure for a particular shell is interpreted from the fact that any further increase in pressure, no matter how small, will cause enormous shell deformation indicating that the state of lowest energy for any increase in pressure is far from that at the critical pressure.

The nonlinear differential equations of shells embodying the principle of minimum potential energy are solved for increasing values of load parameter until the first unstable state of equilibrium is reached. The onset of the first bifurcation point is indicated by a substantial increase in displacements and stresses of the shell for very small increase in the load parameter. At the bifurcation point itself any increase of load parameter, however small, produces enormous deformation and thus the numerical technique used here fails to converge to any solution. It should be noted that the term 'bifurcation point' is used here to refer to the point of initiation of a secondary mode of deformation, may it be limit point or branching point.

Prediction of stability on the basis of purely equilibrium studies is credited in the following two theorems to Thompson.⁹

- **Theorem 1.** An initially stable equilibrium path rising monotonically with the loading parameter cannot become unstable without intersecting a further distinct secondary equilibrium path.
- **Theorem 2.** An initially stable equilibrium path rising with the loading parameter cannot approach an unstable equilibrium state from which the system would exhibit a finite dynamic snap without the approach of an equilibrium path (which may or may not be an extension of the original path) at values of the loading parameter less than that of the unstable state.

Both branching point and limit point buckling of structures are embodied in the instability of the governing large deflection equilibrium equations of these structures. Detection of these points of instability on the primary stable equilibrium path is a handy tool for the study of buckling even

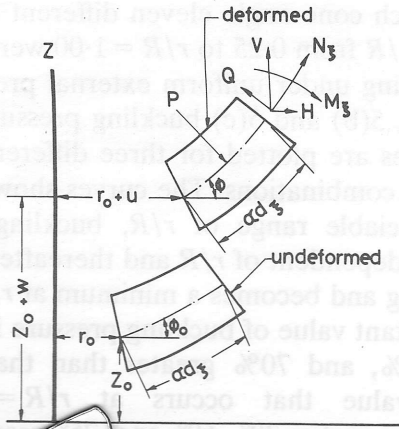


Fig. 2. Side view of elements of shell in deformed and undeformed states.

though it does not specify its type—limit point or branching, symmetric branching or unsymmetric branching, stable branching or unstable branching—all of which depend on the physical parameter of the structure including the boundary restraints and can be answered only after studying the possible postbuckling equilibrium paths.

The nonlinear governing equations used in the present analysis are presented below. The symbols in the equations are defined in Figs 2, 3 and 4.

$$\bar{\epsilon}_\theta = \frac{\bar{u}}{\bar{r}_0} \quad (1a)$$

$$\phi = \phi_0 - \beta \quad (1b)$$

$$\bar{k}_\theta = (\sin \phi_0 - \sin \phi) / \bar{r}_0 \quad (1c)$$

$$\bar{N}_\xi = \bar{H} \cos \phi + \bar{V} \sin \phi \quad (1d)$$

$$\bar{\epsilon}_\xi = \bar{C} \bar{N}_\xi - \nu \bar{\epsilon}_\theta \quad (1e)$$

$$\bar{k}_\xi = \bar{M}_\xi / \bar{D} - \bar{k}_\theta \nu \quad (1f)$$

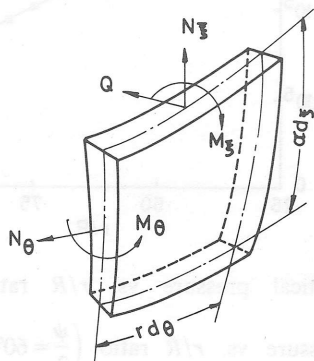


Fig. 3. Elements of shell showing stress resultants and couples.

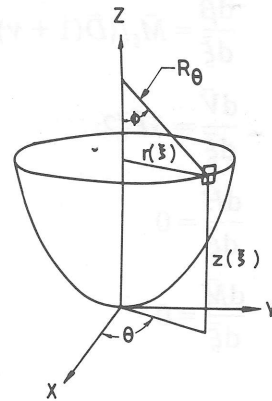


Fig. 4. Middle surface of shell.

$$\bar{N}_\theta = (\bar{\epsilon}_\theta + \nu \bar{\epsilon}_\xi) / \bar{C} \quad (1g)$$

$$\bar{M}_\theta = \bar{D} (\bar{k}_\theta + \nu \bar{k}_\xi) \quad (1h)$$

$$\bar{\alpha} = \bar{L} + \bar{\epsilon}_\xi \quad (1i)$$

$$\bar{r} = \bar{L} \bar{r}_0 + \bar{u} \quad (1j)$$

$$\frac{d\bar{w}}{d\xi} = \bar{\alpha} \sin \phi - \bar{L} \sin \phi_0 \quad (1k)$$

$$\frac{d\bar{u}}{d\xi} = \bar{\alpha} \cos \phi - \bar{L} \cos \phi_0 \quad (1l)$$

$$\frac{d\bar{\beta}}{d\xi} = \bar{k}_\xi \quad (1m)$$

$$\frac{d\bar{V}}{d\xi} = \bar{\alpha} \cos \phi (\bar{V} / \bar{r} - \bar{P} \bar{T}) \quad (1n)$$

$$\frac{d\bar{H}}{d\xi} = -\alpha \{ (\bar{H} \cos \phi - \bar{N}_\theta) / \bar{r} + \bar{P} \bar{T} \sin \phi \} \quad (1o)$$

$$\frac{d\bar{M}}{d\xi} = \bar{\alpha} \cos \phi (\bar{M}_\theta - \bar{M}_\xi) / \bar{r} - \bar{\alpha} \bar{P} \bar{T}^2 \times (\bar{H} \sin \phi - \bar{V} \cos \phi) \quad (1p)$$

The above governing equations are singular at the apex of those shells which are continuous at the apex. When the conditions that all the dependent variables are regular and that the curvature of the undeformed shell is continuous at the apex are imposed, this singularity is removed and the following specialised equations apply at the apex ($\bar{\xi} = 0$).

$$\frac{d\bar{u}}{d\xi} = \bar{C} \bar{H} / (1 + \nu) \quad (2a)$$

$$\frac{d\bar{w}}{d\xi} = 0 \quad (2b)$$

$$\frac{d\bar{\beta}}{d\bar{\xi}} = \bar{M}_{\xi} / \{\bar{D}(1 + \nu)\} \quad (2c)$$

$$\frac{d\bar{V}}{d\bar{\xi}} = \bar{\alpha}\bar{P}/2 \quad (2d)$$

$$\frac{d\bar{H}}{d\bar{\xi}} = 0 \quad (2e)$$

$$\frac{d\bar{M}}{d\bar{\xi}} = 0 \quad (2f)$$

3 BOUNDARY CONDITION

For the general case of axisymmetric deformations of shells of revolution, it was shown in Ref. 6 that the boundary conditions on the edges require specification of \bar{H} or \bar{u} , \bar{M}_{ξ} or β , and \bar{V} or \bar{w} . In the present analysis, the conditions at the centre of the spherical cap become $\bar{u} = 0$, $\beta = 0$, and $\bar{V} = 0$, and that at the base of the shell, where it is considered as a fixed end, they become $\bar{u} = 0$, $\beta = 0$, and $\bar{w} = 0$.

4 SOLUTION

The same method of multisegment integration as used by Uddin⁷ for nonlinear analysis of pressure vessels has been employed with the boundary conditions specified above. To determine the buckling pressure the program starts with an assumed load \bar{P} and a load step $\Delta\bar{P}$, and then solves the nonlinear governing equations at each load step with a preassigned convergence criteria. If the solution fails to converge at any load step, the load step $\Delta\bar{P}$ is automatically halved and the solution is again attempted. When $\Delta\bar{P}$ becomes very small compared to the value of \bar{P} , then \bar{P} is taken as the critical pressure for the buckling of the given shell.

5 RESULTS AND DISCUSSION

Conical frusta of semi-apex angles of 30° , 60° , 75° with $R/h = 100$ are combined with different spherical caps compatible with the corresponding frusta. The combinations studied are shown in Fig. 1. The combination $r/R = 1.0$ is simply a spherical cap compatible with the base radius R of the cone with no conical frustum attached.

For each cone angle eleven different combinations of r/R from 0.25 to $r/R = 1.00$ were studied for buckling under uniform external pressure. In Figs 5(a), 5(b) and 5(c) buckling pressure versus r/R curves are plotted for three different sets of cap/cone combinations. The curves show that for an appreciable range of r/R , buckling load is almost independent of r/R and thereafter it starts decreasing and becomes a minimum at $r/R = 1.0$. The constant value of buckling pressure is around 40%, 50%, and 70% greater than that of the lowest value that occurs at $r/R = 1.0$ for semi-apex angles 30° , 60° and 75° respectively. Thus it seems that the addition of a conical extension to spherical ends may improve the

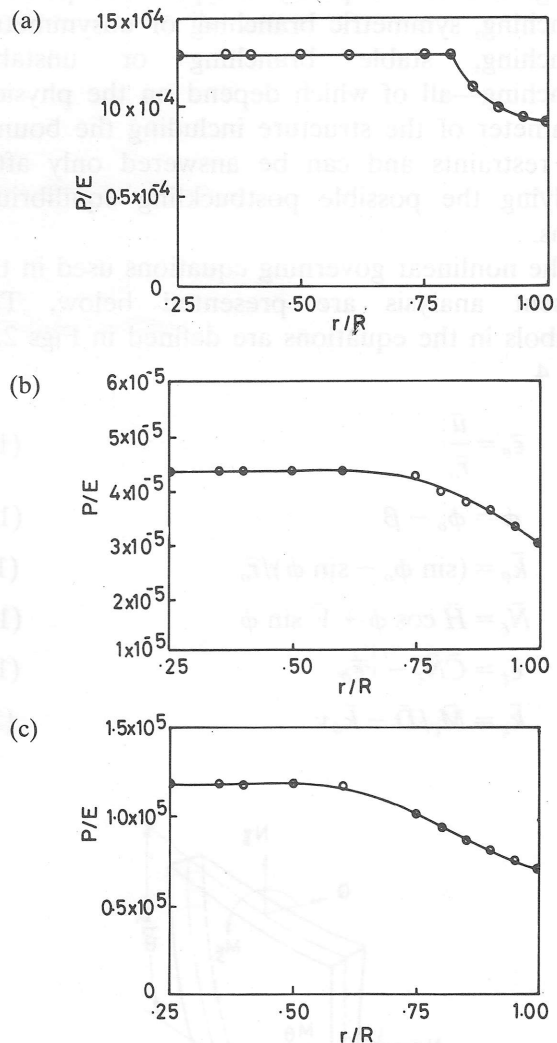


Fig. 5. (a) Critical pressure vs. r/R ratio ($\frac{\psi}{2} = 30^\circ$); (b) critical pressure vs. r/R ratio ($\frac{\psi}{2} = 60^\circ$); (c) critical pressure vs. r/R ratio ($\frac{\psi}{2} = 75^\circ$).

external pressure sustaining capacity of a spherical cap.

In Figs 6–9, the deformed configurations of four shells near critical load with $r/R = 0.25$, 0.50 , 0.75 and 1.00 , and semi-apex angle 30° are shown schematically. The shells in Figs 6, 7 and 8 with conical portion at the base deforms severely near the base only. The deformation pattern of these three shells possesses close similarity. Similarity in buckling load for these three shells may be due to this similar deflection pattern. Figure 9 shows that the simple spherical cap with no conical extension at the vessel end

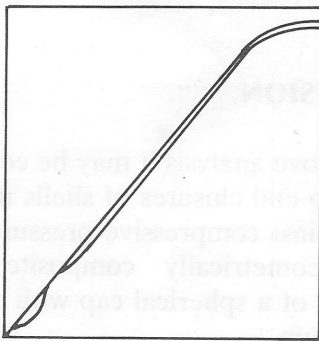


Fig. 6. Shape at critical pressure ($r/R = 0.25$).

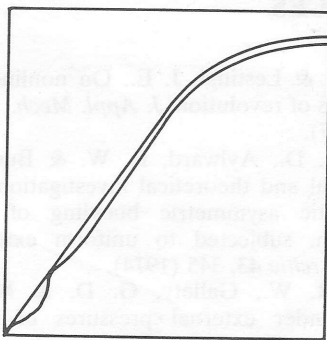


Fig. 7. Shape at critical pressure ($r/R = 0.50$).

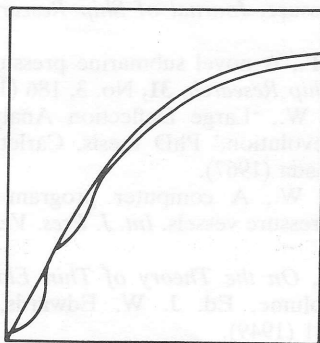


Fig. 8. Shape at critical pressure ($r/R = 0.75$).

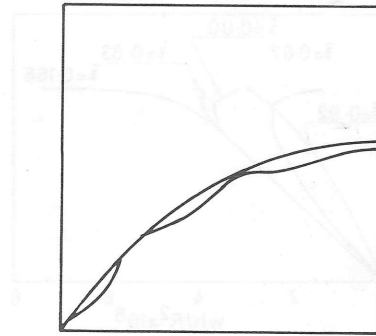


Fig. 9. Shape before load and at critical load ($r/R = 1.0$).

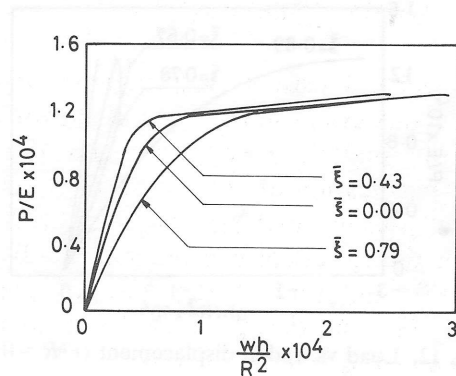
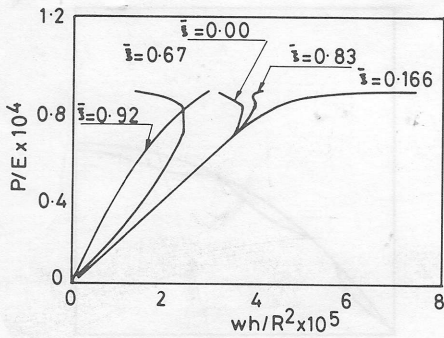
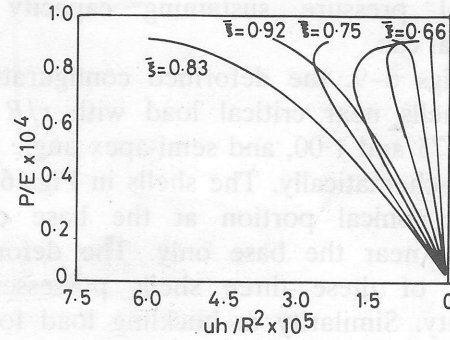
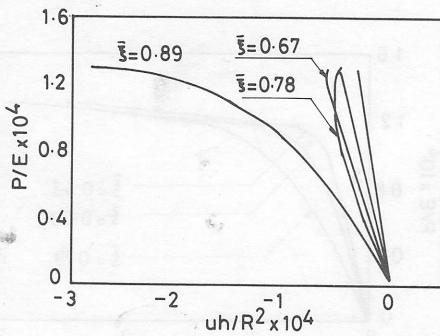
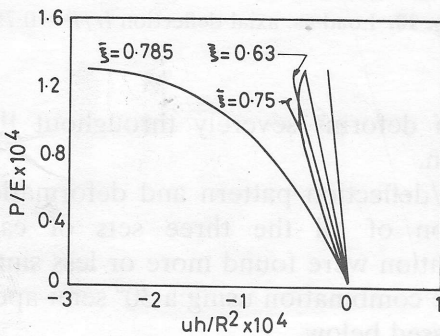
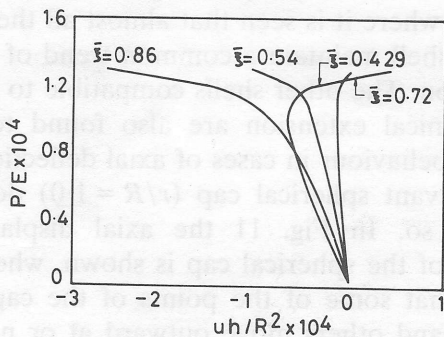


Fig. 10. Load vs. axial deflection ($r/R = 0.75$).

junction deforms severely throughout the shell meridian.

Load/deflection pattern and deformation configuration of all the three sets of cap cone combination were found more or less similar. As such the combination using a 30° semi-apex angle is discussed below.

Load versus axial deflection for the shell with $r/R = 0.75$ and semi-apex angle 30° is shown in Fig. 10, where it is seen that almost all the points on the shell maintain a common trend of inward deflection. The other shells compatible to this set with conical extension are also found to show similar behaviour in cases of axial deflection. But the relevant spherical cap ($r/R = 1.0$) does not behave so. In Fig. 11 the axial displacement history of the spherical cap is shown, where it is found that some of the points of the cap move inward and others move outward at or near the critical load. This kind of behavior is seen in cases of radial displacement of the shells with conical extension, near the base, where radial displacement is severe (Figs 12, 13, 14). Radial deflection of the spherical cap is shown in Fig. 15, which shows that radial displacement of this shell is more or less similar to the other shells.

Fig. 11. Load vs. axial displacement ($r/R = 1.0$).Fig. 15. Load vs. radial displacement ($r/R = 1.0$).Fig. 12. Load vs. radial displacement ($r/R = 0.25$).Fig. 13. Load vs. radial displacement ($r/R = 0.5$).Fig. 14. Load deflection curve for ($r/R = 0.75$).

From the above analysis it is found that a spherical cap under uniform external pressure is much weaker than a cap which is the combination of a spherical cap and a compatible conical frustum. The composite shell is weaker

only near the base, where use of appropriate stiffeners may further improve the load sustaining capacity of the shell.

6 CONCLUSION

From the above analysis it may be concluded that spherical cap end closures of shells may be made stronger against compressive pressure loading by using a geometrically composite shell, the combination of a spherical cap with a compatible conical frustum.

REFERENCES

1. Kalnins, A. & Lestingi, J. E., On nonlinear analysis of elastic shells of revolution, *J. Appl. Mech., Trans. ASME*, **34**, 59 (1967).
2. Gallety, G. D., Aylward, R. W. & Bushnell, D., An experimental and theoretical investigation of elastic and elastic-plastic asymmetric buckling of cylinder-cone combination, subjected to uniform external pressure, *Ingenieur-Archiv* **43**, 345 (1974).
3. Aylward, R. W., Gallety, G. D. & Moffat, D. G., Buckling under external pressures of cylinders with toriconical or pierced torispherical ends: a comparison of experiments with theory, *J. Mech. Eng. Science, I. Mech. E.*, **11** (1975).
4. Ross, C. T. F., Design of dome ends to withstand uniform external pressure, *Journal of Ship Research*, **31**, No. 2, 139 (1987).
5. Ross, C. T. F., A novel submarine pressure hull design. *Journal of Ship Research*, **31**, No. 3, 186 (1987).
6. Uddin, Md. W., 'Large Deflection Analysis of Elastic Shells of Revolution,' PhD thesis, Carleton University, Ottawa, Canada (1967).
7. Uddin, Md. W., A computer program for nonlinear analysis of pressure vessels. *Int. J. Pres. Ves. & Piping* **22**, 271 (1986).
8. Reissner, E., *On the Theory of Thin Elastic Shells*, H. Reissner Volume, Ed. J. W. Edwards, Ann Arbor, Michigan, 231 (1949).
9. Thompson, J. M. T. and Hunt, G. W., *A General Theory of Elastic Stability*. John Wiley and Sons (1973).